(This is a sample cover image for this issue. The actual cover is not yet available at this time.)

Remote Sensing of Environment 128 (2013) 186–196

Contents lists available at SciVerse ScienceDirect

Remote Sensing of Environment

journal homepage: www.elsevier.com/locate/rse

Remote estimation of gross primary productivity in crops using MODIS 250 m data

Yi Peng [a], Anatoly A. Gitelson [a,*], Toshihiro Sakamoto [b]

[a] School of Natural Resources, University of Nebraska-Lincoln, Lincoln, NE, USA
[b] Ecosystem Informatics Division, National Institute for Agro-Environmental Sciences, Tsukuba, Ibaraki, Japan

ARTICLE INFO

Article history:
Received 21 August 2012
Received in revised form 7 October 2012
Accepted 8 October 2012
Available online xxxx

Keywords:
Gross primary productivity
MODIS 250 m data
Vegetation index
Potential photosynthetically active radiation

ABSTRACT

In this study, a simple model was developed to estimate crop gross primary productivity (GPP) using a product of chlorophyll-related vegetation index, retrieved from MODIS 250 m data, and potential photosynthetically active radiation (PAR). Potential PAR is incident photosynthetically active radiation under a condition of minimal atmospheric aerosol loading. This model was proposed for GPP estimation based entirely on satellite data, and it was tested in maize and soybean, which are contrasting crop types different in leaf structures and canopy architectures, under different crop managements and climatic conditions. The model using MODIS 250 m data, which brings high temporal resolution and moderate spatial resolution, was capable of estimating GPP accurately in both irrigated and rainfed croplands in three Nebraska AmeriFlux sites during growing seasons 2001 through 2008. Among the MODIS-250 m retrieved indices tested, enhanced vegetation index (EVI) and wide dynamic range vegetation index (WDRVI) were the most accurate for GPP estimation with coefficients of variation below 20% in maize and 25% in soybean. It was shown that the developed model was able to accurately detect GPP variation in crops where total chlorophyll content is closely tied to seasonal dynamic of GPP.

1. Introduction

Gross primary productivity (GPP) is the total amount of carbon dioxide that is fixed by plants in photosynthesis. Currently approximately 12% of Earth's land surface is cultivated cropland (Wood et al., 2000) and crop GPP contributes approximately 15% of global carbon dioxide fixation (Malmstrom et al., 1997). Thus, accurate and synoptic GPP estimates in crops can provide valuable information for global carbon studies and agricultural applications. Satellite remote sensing is a powerful and expedient tool for assessing crop GPP at regional and global scales, which is essential for estimation of carbon budget and provides objective information for policy decisions related to food security and environmental regulation (Cassman & Wood, 2005).

Many approaches have been developed to assess GPP with remote sensing techniques. Monteith (1972, 1977) suggested that GPP can be expressed as a product of fraction of absorbed photosynthetically active radiation (fAPAR), incident photosynthetically active radiation (PAR_{in}) and light use efficiency (LUE), which is the efficiency of the absorbed PAR converted into biomass. Based on this concept, fAPAR was approximated by the normalized difference vegetation index — NDVI (Rouse et al., 1974), which can be retrieved from satellite data. LUE is commonly regarded as a near constant value. The problems of such approaches are: (a) a significant decrease in the sensitivity of NDVI to moderate-to-high vegetation density when fAPAR exceeds 0.7, which is typical for crops (e.g., Asrar et al., 1984; Gitelson et al., 2006; Kanemasu, 1974; Viña & Gitelson, 2005), and (b) the species-specific rather than the merely biome-specific variation of LUE (e.g., Ahl et al., 2004; Ruimy et al., 1994). In order to account for the variations of LUE, some remote sensing models use look-up tables of maximum LUE for specific vegetation types, and these values are then adjusted downward by considering environmental stress factors (Anderson et al., 2000; Ruimy et al., 1994; Running et al., 2004; Xiao et al., 2004b; Yuan et al., 2007). The photochemical reflectance index (PRI) was proposed as a proxy of LUE at different scales from leaves to entire canopies (Gamon et al., 1992). However, a model that can effectively explain the variation of LUE, resulting in a significant increase in the accuracy of GPP estimation, is yet to be developed.

Another approach is to estimate GPP by using process-based models (e.g., Potter et al., 1993; Xiao et al., 2004a, 2011). Numerical schemes were developed to integrate different data types: remote sensing data, daily meteorological data, and soil data grouped in polygons (e.g., Liu et al., 1997). This approach requires estimates of canopy light absorption or leaf area index that can be retrieved from satellite data, as well as spatial data on climate, topography and soil physical characteristics. The daily meteorological data usually includes air temperature, incoming shortwave radiation, precipitation, and humidity. The soil-data input indicates the available water-holding capacity. This approach was successfully used for estimating GPP of different vegetation types, however, it requires a lot of ancillary data for accurate GPP estimation.

* Corresponding author. Tel.: +1 402 4728386; fax: +1 402 4724608.
E-mail address: agitelson2@unl.edu (A.A. Gitelson).

0034-4257/$ – see front matter © 2012 Elsevier Inc. All rights reserved.
http://dx.doi.org/10.1016/j.rse.2012.10.005

Since total canopy chlorophyll (Chl) content was found to be a very direct expression of the photosynthetic apparatus of a plant community (Medina & Lieth, 1964; Whittaker & Marks, 1975), especially in croplands where total Chl content closely follows the dynamic of GPP (Osborne & Raven, 1986), a paradigm was developed to assess crop GPP via the estimation of total crop Chl content (Gitelson et al., 2003, 2006). Based on this paradigm, several approaches have been developed to estimate GPP using satellite data. Using Medium Resolution Imaging Spectrometer (MERIS) data, MERIS terrestrial chlorophyll index (MTCI) was tested for evaluating GPP across a variety of land cover and vegetation types, and it showed great potential for estimating GPP in croplands, grassland and deciduous forest (Almond et al., 2010; Harris & Dash, 2010; Wu et al., 2009). Xiao et al. (2004b) assessed GPP of U.S. terrestrial ecosystems with Moderate Resolution Imaging Spectroradiometer (MODIS) vegetation index (VI) products as indicators of vegetation Chl content and auxiliary climate data. Gitelson et al. (2008) estimated crop GPP by employing Chl-related VI retrieved from Landsat ETM + images.

A simple model was suggested to relate crop GPP to a product of Chl-related VI and incoming photosynthetic radiation (PAR_{in}) — $GPP \propto VI \times PAR_{in}$ (Gitelson et al., 2006; Peng et al., 2011). It was shown that the VI-PAR_{in}-based model was able to accurately estimate GPP in crops using MODIS data (Wu et al., 2010, 2011), as well as MERIS data (Boyd et al., 2012). However, this model requires PAR_{in} ancillary data. Sakamoto et al. (2011, 2010) estimated GPP using solely remotely sensed data with MODIS-retrieved wide dynamic range vegetation index (WDRVI), as a proxy of total Chl content, and shortwave radiation (SW) data of NASA reanalysis dataset (North American Land Data Assimilation System, NLDAS-2) as a substitute for PAR_{in} — $GPP \propto WDRVI \times SW$. The model was able to accurately estimate GPP in maize croplands. However, SW, retrieved from NLDAS-2, and ground observed PAR_{in} are not closely related and there is a potential for significant uncertainties of GPP estimation (Sakamoto et al., 2011, 2010).

Gitelson et al. (2012) suggested using a product of Chl-related VI and potential photosynthetic active radiation ($PAR_{potential}$) — $GPP \propto VI \times PAR_{potential}$ for estimating crop GPP. $PAR_{potential}$ is PAR_{in} under conditions of minimal aerosol loadings and represents the seasonal changes in hours of sunshine (i.e. day length). It was not suggested as a substitute for PAR_{in} but rather as a better than PAR_{in} representative of incident radiation affecting crop photosynthesis. The model is based solely on remotely sensed data since $PAR_{potential}$ could be calculated using the 6S radiative transfer code (Vermote et al., 1997) for a "clean" (non- absorbing) aerosol model with optical thickness of 0.05 at 550 nm and water vapor below 1 g/m^2. The solar irradiance at the top of the atmosphere, geographic coordinates and solar angle for a given location should be used as input data (Kotchenova & Vermote, 2007). Another way to get $PAR_{potential}$ is to use a look-up table (LUT)-based algorithm (Lyapustin, 2003), providing PAR_{in} as a function of solar zenith angle, column water vapor and optical thickness for several different representative aerosol models.

The model using $PAR_{potential}$ was applied to estimate GPP accurately in irrigated and rainfed maize–soybean croplands during an 8-year period with Landsat data, and appeared to be superior to the VI-PAR_{in}-based model (Gitelson et al., 2012). However, poor temporal resolution of Landsat data (one scene per 16 days, only 4–10 images per growing season in Nebraska) may be an issue for environmental monitoring.

In order to monitor crop dynamics more frequently, one needs to turn to satellite data with much higher than Landsat temporal resolution. The MODIS 250 m products with high temporal resolution have been increasingly used for crop mapping and monitoring. It provides daily observations for the globe, and it is feasible to provide reliable spatial information for typical size of cropped fields in North America. Since the VI-$PAR_{potential}$-based model has been successfully applied to Landsat data to estimate GPP in croplands, it is necessary to explore the potential of applying this model to MODIS 250 m data to monitor crop GPP with high temporal resolution.

The objectives of this study are: (1) to test performance of the VI-$PAR_{potential}$-based model for estimating GPP in irrigated and rainfed maize–soybean croplands using MODIS 250 m data; (2) to examine and compare uncertainties of the models for GPP estimation with $PAR_{potential}$, PAR_{in} and SW (retrieved from NLDAS-2); and (3) to evaluate the sensitivity of the chlorophyll-based model to estimate GPP of water-stressed crops.

2. Data and methods

2.1. Study sites

In this investigation, the data from three AmeriFlux sites located at the University of Nebraska-Lincoln Agricultural Research and Development Center near Mead, Nebraska (NE), USA, were studied during eight growing seasons from 2001 through 2008. These three sites are all approximately 60-ha fields located 1.6 km of each other. Site 1 (Us-Ne1: public.ornl.gov/ameriflux/Site_Info/siteInfo.cfm?KEYID=us.mead_maize.01) is planted in continuous maize equipped with a center pivot irrigation system. Site 2 (Us-Ne2: public.ornl.gov/ameriflux/Site_Info/siteInfo.cfm?KEYID=us.mead_maize_soybean_irrigated.01) and site 3 (Us-Ne3: public.ornl.gov/ameriflux/Site_Info/siteInfo.cfm?KEYID=us.mead_maize_soybean_rainfed.01) are both planted in maize–soybean rotation and maize was planted in odd years. Site 2 is irrigated in the same way as site 1, while site 3 relies entirely on rainfall for moisture. More details about the crop management and field history of these study sites are available in Verma et al. (2005).

2.2. Eddy covariance GPP flux measurements

Each study site was equipped with an eddy covariance tower and meteorological sensors, with which the continuous measurements of CO_2 fluxes, water vapor and energy fluxes were obtained every hour. Daytime net ecosystem exchange (NEE) values were computed by integrating the hourly CO_2 fluxes collected during a day when PAR_{in} exceeded 1 $\mu mol/m^2/s$. Daytime estimates of ecosystem respiration (Re) were obtained from the night CO_2 exchange–temperature relationship (e.g., Xu & Baldocchi, 2003). The GPP was then obtained by subtracting Re from NEE as: GPP = NEE − Re. GPP values were presented in the unit of $gC/m^2/d$, and the sign convention used here was such that CO_2 flux to the surface was positive so that GPP was always positive and Re was always negative (Verma et al., 2005).

2.3. Ground-observed incoming PAR

Point quantum sensors (LI-190, LI-COR Inc., Lincoln, Nebraska) were placed in each study site, 6 m above the surface pointing toward the sky, to measure hourly incoming PAR (PAR_{in}). Daytime PAR_{in} values were computed by integrating the hourly measurements during a day when PAR_{in} exceeded 1 $\mu mol/m^2/s$. Daily PAR_{in} values were presented in $MJ/m^2/d$ (Turner et al., 2003).

2.4. Potential PAR

Potential PAR ($PAR_{potential}$) is the maximal value of PAR_{in} that may occur when the concentrations of atmospheric gases and aerosols are minimal (Gitelson et al., 2012). Representing the seasonal changes in hours of sunshine (i.e. day length), $PAR_{potential}$ does not account for high frequency variation of incoming radiation related to daily weather conditions. In this study, we calculated $PAR_{potential}$ using ground-observed PAR_{in} values. Since the daylight duration is mainly determined by the day of a year (DOY) and geographic location, we created profiles of $PAR_{potential}$ as functions of DOY for sites located in

Nebraska, based on daytime PAR_{in} obtained during 2001–2008. For each DOY, a maximal PAR_{in} value was found in the 8-day-PAR_{in} window centered on that particular DOY. The best-fit functions of the relationships between maximal PAR_{in} and DOY were found for each year and the variation among the years was very small (coefficient of variation below 3.5% — Gitelson et al., 2012; Peng, 2012). Thus, the $PAR_{potential}$ was calculated as the maximal PAR_{in} value for each DOY during an 8 year period.

2.5. Shortwave radiation

The spectral range of shortwave radiation (SW) is 300–4000 nm: it includes specific bands of water vapor absorption and PAR (400–700 nm). Following Sakamoto et al. (2011, 2010), the daily SW data of the reanalysis dataset (North American Land Data Assimilation System, NLDAS-2) was used as a proxy of PAR_{in}. The footprint of one SW pixel (spatial resolution: 1/8°, ca. 11 km at the sites) covers all three Nebraska sites. NLDAS-2 land-surface forcing files are derived from the analysis fields of the National Centers for Environmental Prediction (NCEP) North American Regional Reanalysis (Fang, 2009). There is a close relationship between PAR_{in}, retrieved from the reanalysis SW data, and observed PAR_{in} with determination coefficients $R^2 = 0.76$ (Sakamoto et al., 2011, 2010). Thus, it seemed reasonable to substitute SW for PAR_{in} observations to detect the high frequency variation of incoming light intensity.

2.6. Vegetation indices retrieved from MODIS 250 m data

A MODIS pixel located near the center of each flux site was used to represent the footprint. Due to limited spectral resolution (only red and NIR bands are available in MODIS 250 m data), three Chl-related VIs were examined in this study: NDVI (Rouse et al., 1974), EVI (Huete et al., 1997) and WDRVI (Gitelson, 2004). MODIS NDVI was retrieved from MODIS 250 m surface reflectance data (MOD09Q1). EVI was calculated using NIR and red reflectance of MOD09Q1 with blue reflectance of MOD0A1 (500 m resolution), which was resampled with the nearest neighbor method to 250 m resolution:

$$EVI = (\rho_{NIR} - \rho_{Red})/(\rho_{NIR} + 6 \times \rho_{Red} - 7.5 \times \rho_{blue} + 1).$$

MODIS WDRVI was calculated using MODIS NDVI product as (Viña & Gitelson, 2005):

$$WDRVI = [(\alpha - 1) + (\alpha + 1) \times NDVI]/[(\alpha + 1) + (\alpha - 1) \times NDVI].$$

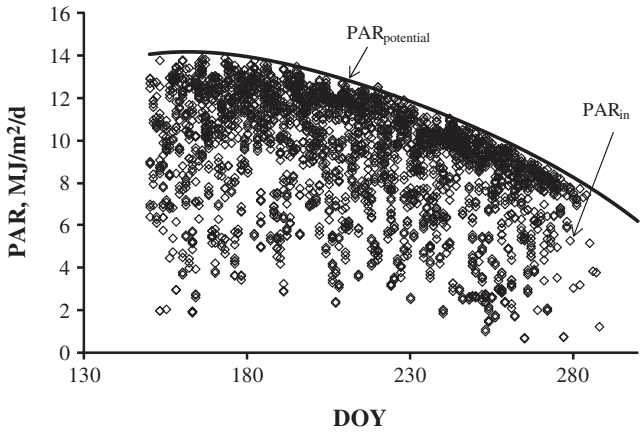

Fig. 1. Temporal behavior of daily PAR_{in} and the $PAR_{potential}$ profile (solid line) during the growing seasons 2001 through 2008 created for Mead, Nebraska.

Since WDRVI may be negative for low vegetation density, in this study, we used scaled WDRVI (Peng & Gitelson, 2011) with, $\alpha = 0.3$, which ranged from 0 to 1.56:

$$\text{Scaled WDRVI} = [(\alpha - 1) + (\alpha + 1) \times NDVI]/[(\alpha + 1) + (\alpha - 1) \times NDVI] + (1 - \alpha)/(1 + \alpha).$$

Even though the surface reflectance used to calculate the VIs were atmospherically corrected, the observed VI time-series were liable to include various residual noise components resulting in an erratic time series behavior and many sharp spikes in VI values. In addition, observational day of time-series VIs, derived from MODIS-8-day composite products, was not recorded in regular intervals. Therefore, a wavelet-based filter was applied for removing the high-frequency noise components to produce a daily smoothed VI profiles in the same manner as Sakamoto et al. (2011, 2010). In the preprocessing scheme, the potential cloud-covered pixels were detected by blue reflectance (as it was greater than 0.2). This threshold of blue reflectance was established empirically and widely used (e.g., Sakamoto et al., 2007; Thenkabail et al., 2005; Xiao et al., 2006). Then, available observations were linearly interpolated in reference to the observation-date data recorded in MOD09A1 product.

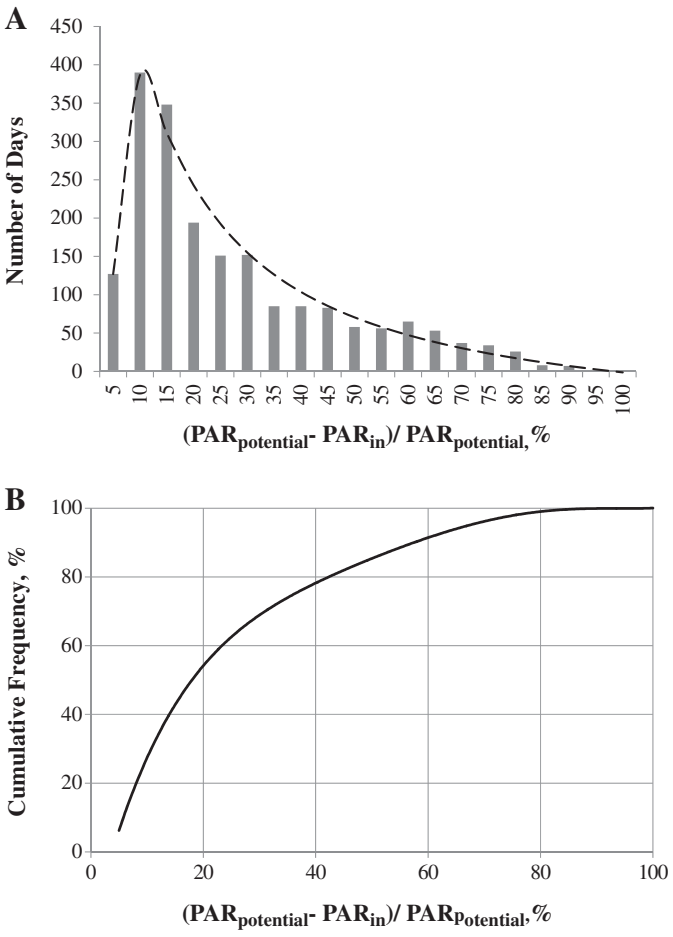

Fig. 2. Number of days (A) and cumulative frequency distribution (B) plotted versus the difference between PAR_{in} and $PAR_{potential}$, $(PAR_{potential} - PAR_{in})/PAR_{potential}$, for Mead, Nebraska during growing seasons 2001 through 2008. For 55% of observations during growing seasons the difference between PAR_{in} and $PAR_{potential}$ was below 20% and for about 80% of observations the difference was below 40%.

3. Results and discussion

3.1. $PAR_{potential}$ and PAR_{in} on daily basis

The ground-observed daily PAR_{in} values and the $PAR_{potential}$ profile created for Nebraska sites during the growing seasons 2001 through 2008 are shown in Fig. 1, and the histogram of the difference of PAR_{in} and $PAR_{potential}$, $(PAR_{potential} - PAR_{in})/PAR_{potential}$, is presented in Fig. 2A. The eastern part of Nebraska (e.g. study sites in Mead) has a humid continental climate, with hot and sunny summers, which are the main growing seasons for maize and soybean. 1554 out of 2834 days during eight growing seasons were under clear atmospheric conditions with $(PAR_{potential} - PAR_{in})/PAR_{potential}$ smaller than 20%, as were the conditions for most Landsat acquisition dates over the same area (Gitelson et al., 2012). The images taken at such days may be qualified for providing good pixel reflectance values to 8-day MODIS composite product. 2235 out of 2834 days during eight growing seasons were in condition of $(PAR_{potential} - PAR_{in})/PAR_{potential}$ lower than 40%, as was the maximum difference between PAR_{in} and $PAR_{potential}$ that occurred for Landsat acquisition dates during the same period (Gitelson et al., 2012). In the Landsat dataset, collected over an 8 year period, only few clear images were acquired during the growing season (4–10 images, less than 9% of the daily-smoothed MODIS dataset). In contrast, as shown in Fig. 2B for daily-smoothed MODIS data, 55% of MODIS images were obtained when $(PAR_{potential} - PAR_{in})/PAR_{potential}$ was below 20%, and 78% of images were obtained when $(PAR_{potential} - PAR_{in})/PAR_{potential}$ was below 40%. Thus, as expected, the information content of MODIS 250 data was much higher than that of Landsat data.

3.2. GPP estimation by the product of VI and PAR_{in}, SW and $PAR_{potential}$

The relationships between GPP and the products of $VI \times PAR_{in}$, $VI \times SW$ and $VI \times PAR_{potential}$, established for Nebraska sites on days when $(PAR_{potential} - PAR_{in})/PAR_{potential}$ was below 20% during growing seasons 2001 through 2008 are presented in Fig. 3. In both maize and soybean, the relationships were close with determination coefficient (R^2) above 0.87 for maize and 0.78 for soybean. For all three models using PAR_{in}, SW and $PAR_{potential}$, the best-fit functions NDVI vs. GPP were nonlinear, while they were linear for EVI and WDRVI. The value of R^2 may be misleading when the best fit function is nonlinear, because it represents only the overall dispersion of the points from the regression line regardless of shapes of relationships (Nguy-Robertson et al., 2012; Viña & Gitelson, 2005). As shown in Fig. 3, the models with NDVI tended to be saturated as GPP exceeded 20 $gC/m^2/d$ in maize and 10 $gC/m^2/d$ in soybean. The sensitivity of the models that used NDVI decreased drastically as GPP increased: for almost the same value of the products of NDVI and PAR_{in}, SW or

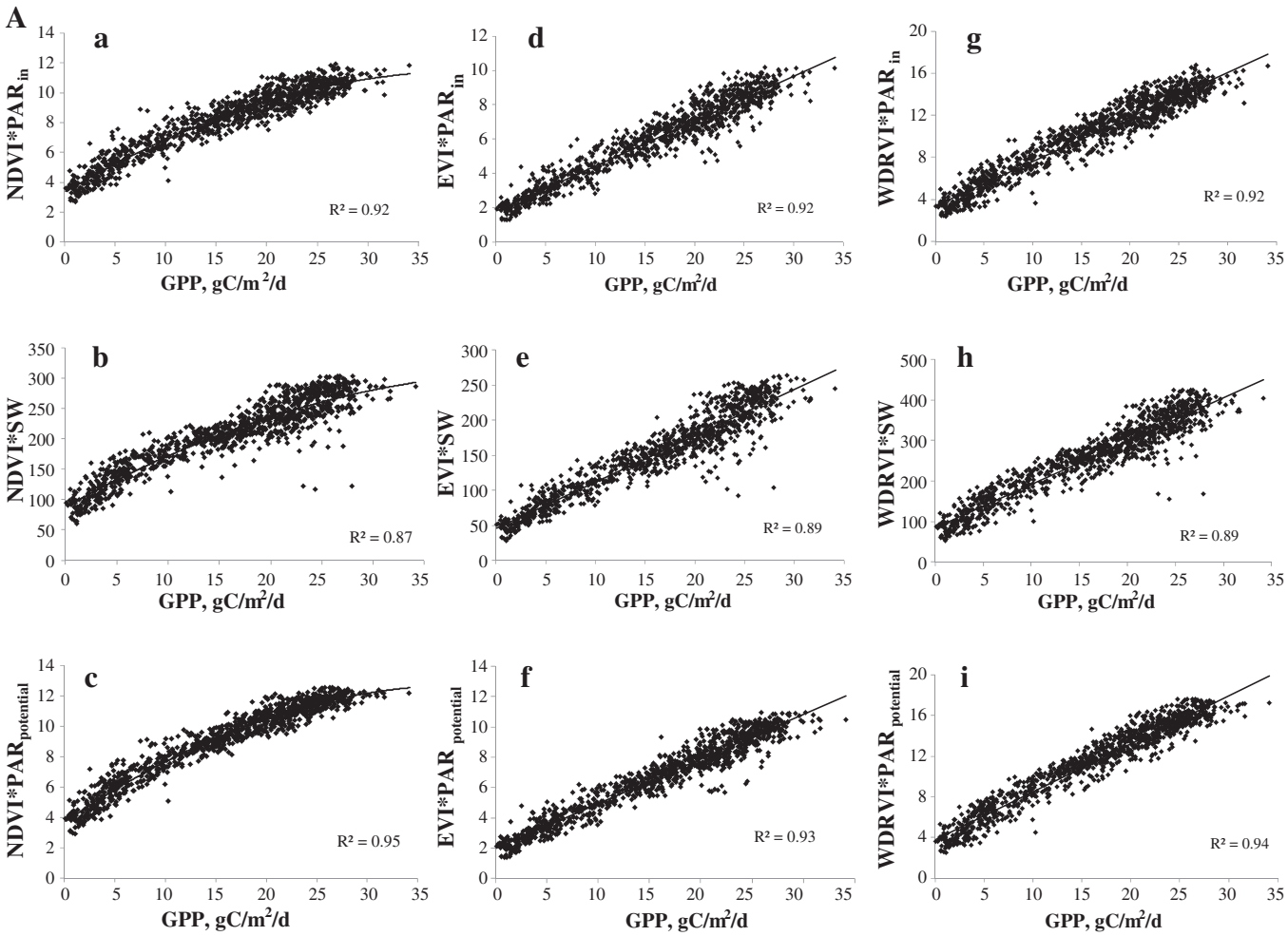

Fig. 3A. The product of (a) $NDVI \times PAR_{in}$, (b) $NDVI \times SW$, (c) $NDVI \times PAR_{potential}$, (d) $EVI \times PAR_{in}$, (e) $EVI \times SW$, (f) $EVI \times PAR_{potential}$, (g) $WDRVI \times PAR_{in}$, (h) $WDRVI \times SW$ and (i) $WDRVI \times PAR_{potential}$ plotted versus GPP for observations during growing seasons 2001 through 2008 in Nebraska maize sites when $(PAR_{potential} - PAR_{in})/PAR_{potential}$ was below 20%. Vegetation indices were retrieved from MODIS 250 m data. B. The product of (a) $NDVI \times PAR_{in}$, (b) $NDVI \times SW$, (c) $NDVI \times PAR_{potential}$, (d) $EVI \times PAR_{in}$, (e) $EVI \times SW$, (f) $EVI \times PAR_{potential}$, (g) $WDRVI \times PAR_{in}$, (h) $WDRVI \times SW$ and (i) $WDRVI \times PAR_{potential}$ plotted versus GPP for observations during growing seasons 2001 through 2008 in Nebraska soybean sites when $(PAR_{potential} - PAR_{in})/PAR_{potential}$ was below 20%. Vegetation indices were retrieved from MODIS 250 m data.

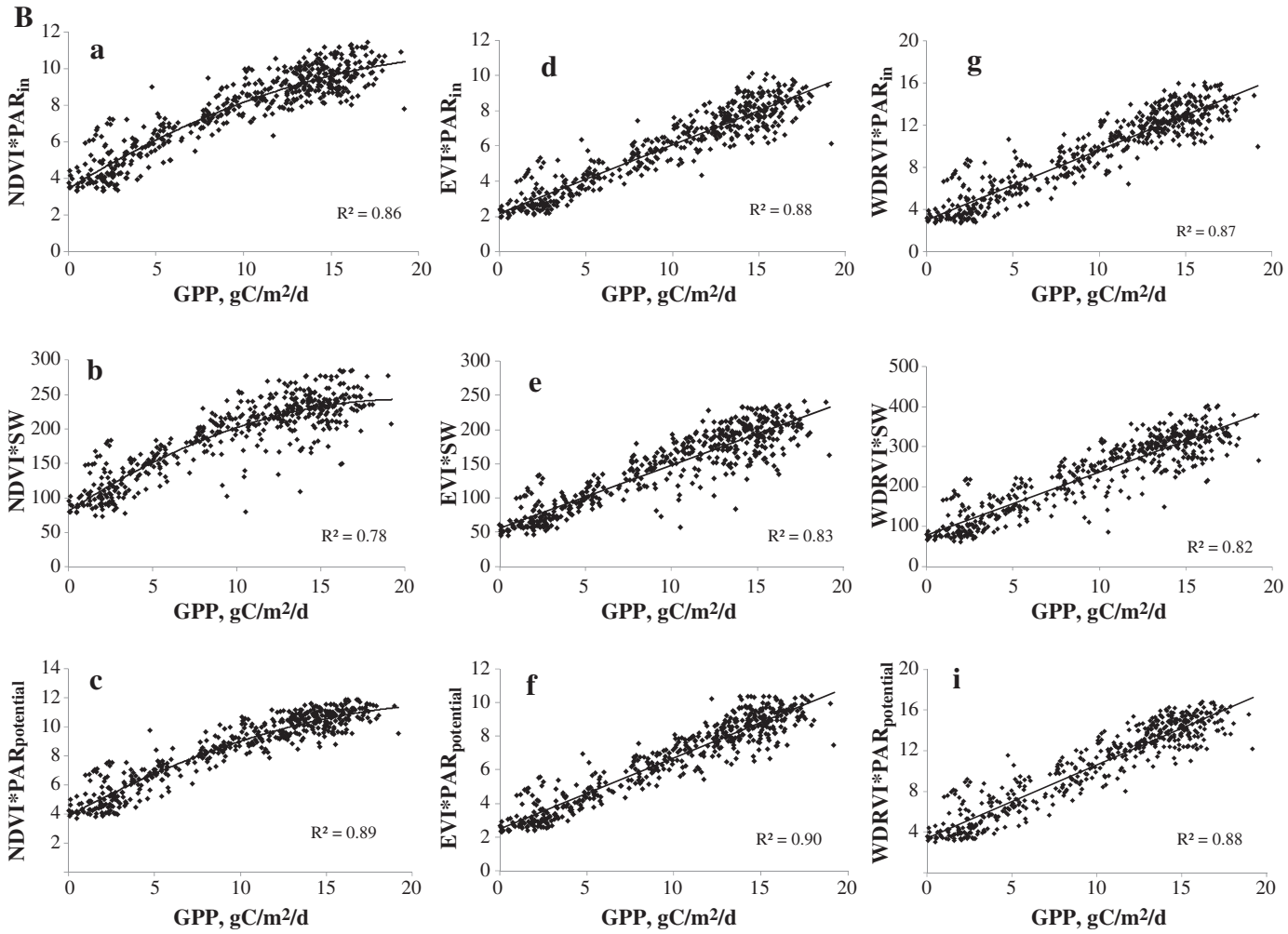

Fig. 3B. The product of (a) NDVI × PAR_{in}, (b) NDVI × SW, (c) NDVI × $PAR_{potential}$, (d) EVI × PAR_{in}, (e) EVI × SW, (f) EVI × $PAR_{potential}$, (g) WDRVI × PAR_{in}, (h) WDRVI × SW and (i) WDRVI × $PAR_{potential}$ plotted versus GPP for observations during growing seasons 2001 through 2008 in Nebraska soybean sites when (PARpotential−PARin)/PARpotential was below 20%. Vegetation indices were retrieved from MODIS 250 m data.

$PAR_{potential}$, GPP ranged from 20 to 30 gC/m^2/d in maize and from 13 to 20 gC/m^2/d in soybean.

The accuracy of GPP estimation using NDVI, EVI and WDRVI was assessed in terms of noise equivalent (NEΔGPP) calculated as (Viña & Gitelson, 2005):

$$NE\Delta GPP = SE\{VI \times PARvs.GPP\}/d(VI \times PAR)/d(GPP)$$

where SE{VI × PAR vs. GPP} is the standard error (SE) of the relationship VI × PAR vs. GPP, and d(VI × PAR)/d(GPP) is the first derivative of VI × PAR with respect to GPP. This metric considers both the shape and scattering of the points of the best fit relationship (Viña & Gitelson, 2005; Viña et al., 2011). NDVI was most accurate in estimating low GPP values (below 15 gC/m^2/d in maize and below 10 gC/m^2/d in soybean), but became less sensitive to moderate-to-high GPP. The NE ΔGPP of NDVI increased hyperbolically at least two-fold when GPP was above 25 gC/m^2/d in maize and 15 gC/m^2/d in soybean (Fig. 4). Models with EVI and WDRVI remained sensitive to the whole range of GPP variation (constant NEΔGPP values), and they were more accurate than NDVI in estimating moderate to high GPP.

It is also worth noting that for all three models, the accuracy of GPP estimation in soybean was lower than in maize (Figs. 3 and 5). This is consistent with the observation using Landsat data, which was explained by hysteresis of GPP/PAR vs. NIR reflectance relationship (details in Gitelson et al., 2012).

Determination coefficients R^2 were high for all three models using SW, PAR_{in} and $PAR_{potential}$. However, for all three indices tested in this study, in both maize and soybean, the R^2 was lower when using VI × SW than VI × PAR_{in} or VI × $PAR_{potential}$ (R^2 was 0.89 vs. 0.92 for maize, and 0.83 vs. 0.88 for soybean). VI × $PAR_{potential}$ and VI × PAR_{in} were both closely related to GPP with the former performing slightly better (Fig. 3).

EVI and WDRVI appeared to be the best indices for GPP estimation. The accuracy of three models, GPP = VI × $PAR_{potential}$, GPP = VI × PAR_{in} and GPP = VI × SW, for GPP estimation using EVI and WDRVI were compared (Tables 1a and 1b, Fig. 5). The model with SW was substantially less accurate than the model with $PAR_{potential}$ or PAR_{in}. This is due to the uncertainties of using SW as a proxy of PAR_{in} in the model (Sakamoto et al., 2011, 2010), which has many outliers (Fig. 3), thus, much higher SE and CV values.

For both indices, EVI and WDRVI, the model with $PAR_{potential}$ was consistently more accurate than the model with PAR_{in}: the model using PAR_{in} had at least 6% higher SE for EVI in soybean (1.86 vs. 1.75 gC/m^2/d) and more than 15% higher SE for WDRVI in maize (2.31 vs. 2.04 gC/m^2/d) — Tables 1a and 1b. This is in accord with results obtained from Landsat data over the same sites (Gitelson et al., 2012).

3.3. GPP estimation in water-stressed crops

The VI-PAR-based models were developed for assessing vegetation GPP via estimation of total canopy Chl content by using VI related

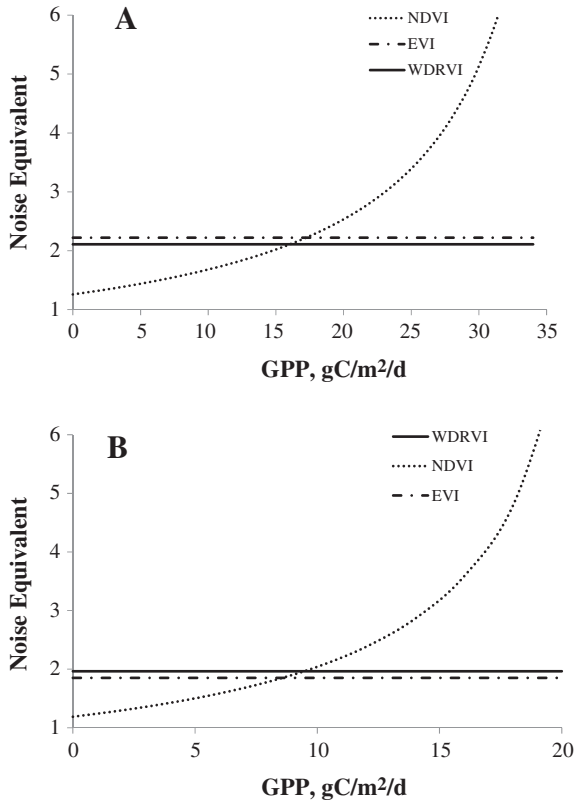

Fig. 4. The Noise Equivalent (NEΔGPP) of GPP estimation using models with NDVI, WDRVI and EVI for (A) maize and (B) soybean.

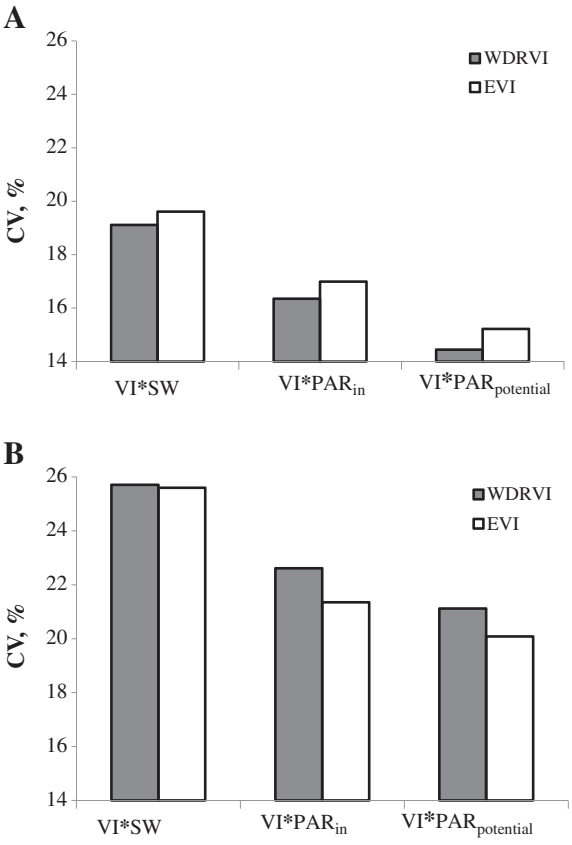

Fig. 5. Coefficients of variation (CV) of GPP estimation using VI×SW, VI×PAR_{in} and VI×$PAR_{potential}$ using EVI and WDRVI in (A) maize and (B) soybean.

Table 1a
Relationships: GPP vs. VI∗PAR_{in}, GPP vs. VI∗SW and GPP vs. VI∗$PAR_{potential}$ with WDRVI and EVI, established for maize sites in Mead, Nebraska during 2001 through 2008 on days when ($PAR_{potential}$ − PAR_{in})/$PAR_{potential}$ was below 20%. Best fit functions, determination coefficients (R^2) and standard errors (SE) are presented. Maize GPP ranged from 0 to 30 gC/m^2/d.

Model	GPP = VI × SW	GPP = VI × PAR_{in}	GPP = VI × $PAR_{potential}$
WDRVI			
Best fit function	GPP = 0.08x − 5.40	GPP = 0.42x + 3.39	GPP = 0.47x + 3.78
R^2	0.89	0.92	0.94
SE, gC/m^2/d	2.70	2.31	2.04
EVI			
Best fit function	GPP = 0.13x − 4.17	GPP = 3.49x − 4.92	GPP = 3.18x − 5.29
R^2	0.89	0.92	0.93
SE, gC/m^2/d	2.77	2.40	2.15

to canopy Chl content. Such models do not account for the short-term (minutes to hours) environmental stresses (e.g., temperature, humidity, and soil moisture, among others), which may not immediately affect the canopy Chl content but may affect GPP. Such kind of stresses cannot be estimated using MODIS daily data. However, it was shown that MODIS data allowed estimating day-to-day crop GPP variation (e.g., Sakamoto et al., 2011, 2010). We examined the sensitivity of the VI-$PAR_{potential}$-based model to detect response of maize daily GPP to water deficiency, analyzing the performance of the model in irrigated and rainfed maize fields. Year 2003 had significant drought periods from DOY (day of year) 199 to 209 and from DOY 216 to 272 (Suyker & Verma, 2010). In July and August, the precipitation was 60 mm/month below normal, and the air temperature during these two months was higher than normal: 0.8 °C higher in July and 1.9 °C higher in August (Suyker & Verma, 2010). The studied irrigated and rainfed sites were within 1.6 km of each other, thus, the concurrent measurements in these two sites were taken under the same climate and illumination conditions. So, the water supply was the major difference between these irrigated and rainfed sites.

As shown in Fig. 6A, measured GPP values in the irrigated and rainfed sites were very close from DOY 150 to 190 when no water stress was detected (Suyker & Verma, 2010). As the drought period began (around DOY 200), the soil moisture at the depth of 10 cm in the rainfed site sharply decreased by more than 30% (from 0.42 m^3/m^3 to 0.22 m^3/m^3), and GPP in the rainfed site became lower than in the irrigated site. This discrepancy between GPP in the irrigated and rainfed sites became significant during the dry period DOY

Table 1b
Relationships: GPP∝VI∗PAR_{in}, GPP∝VI∗SW and GPP∝VI∗$PAR_{potential}$ with WDRVI and EVI, established for soybean in Mead, Nebraska during 2001 through 2008 on days when ($PAR_{potential}$ − PAR_{in})/$PAR_{potential}$ was below 20%. Best fit functions, determination coefficients (R^2) and standard errors (SE) were given. Soybean GPP ranged from 0 to 20 gC/m^2/d.

Model	GPP = VI × SW	GPP = VI × PAR_{in}	GPP = VI × $PAR_{potential}$
WDRVI			
Best fit function	GPP = 0.05x − 2.3	GPP = 1.31x − 2.69	GPP = 1.22x − 3.04
R^2	0.82	0.87	0.88
SE, gC/m^2/d	2.24	1.97	1.84
EVI			
Best fit function	GPP = 0.09x − 3.22	GPP = 2.26x − 3.73	GPP = 2.11x − 4.12
R^2	0.83	0.88	0.90
SE, gC/m^2/d	2.23	1.86	1.75

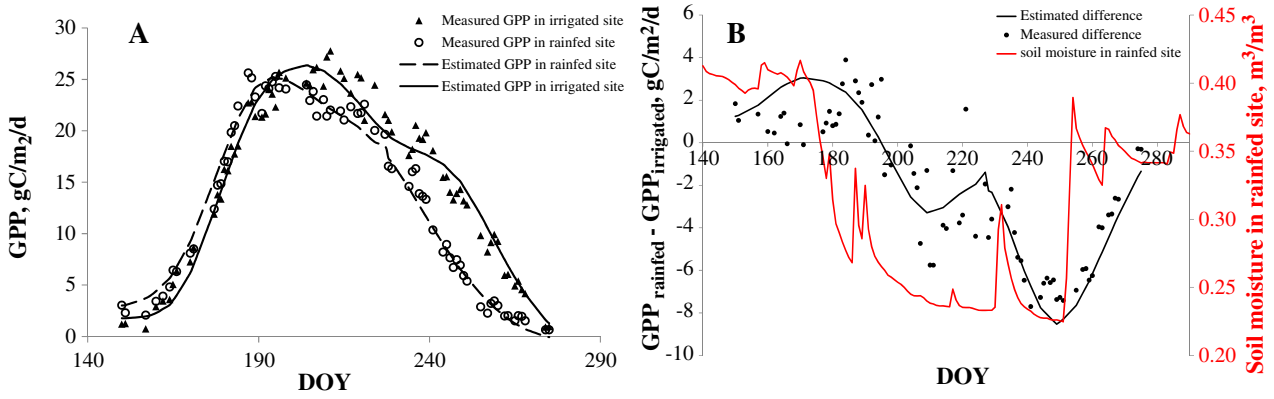

Fig. 6. (A) Measured and estimated (as WDRVI × $PAR_{potential}$) GPP in the irrigated and the rainfed sites. (B) The difference between GPP measured and estimated by the model WDRVI × $PAR_{potential}$ in the irrigated and rainfed sites and soil moisture at the depth of 10 cm in the rainfed site, plotted versus DOY (day of year) in 2003. The model demonstrated high sensitivity to differences in GPP between irrigated and rainfed sites in the drought period (DOY 200–250) when soil moisture in the rainfed site was low.

240–250 when soil moisture in the rainfed site remained very low for more than one month and the highest water stress (represented by the difference between irrigated and rainfed evaporative fraction — Suyker & Verma, 2010) was detected. Importantly, during the growing season, GPP estimated by the model WDRVI × $PAR_{potential}$ closely followed measured GPP, and the estimated GPP had patterns very similar to that of measured GPP in both sites (Fig. 6A).

To further explore the sensitivity of the model to GPP variation, caused by water stress, the differences between measured and estimated (by VI × $PAR_{potential}$) GPP in the irrigated and rainfed fields were plotted versus DOY (Fig. 6B). The model demonstrated ability to detect differences in daily GPP between irrigated and rainfed sites even in the very beginning of the drought period (around DOY 200) at early stage of stress. This may be valid not only for crop systems, but also for ecosystems where vegetation greenness is closely tied to seasonal dynamic of GPP and total Chl content is a dominant factor of GPP (e.g., Garbulsky et al., 2011; Gitelson et al., 2006; Peng et al., 2011).

Fig. 6B shows also that early in the growing season (DOY 150 to 180), the GPP value, estimated by the model in the rainfed site, was higher than in the irrigated site, while during this period the measured GPP values were almost the same in these two sites. One of the reasons for that may be the different density of planting in irrigated and rainfed sites. The density of planting in the rainfed site was at least 25% lower than in the irrigated site. Early in the season with low to moderate vegetation fraction (30% to 50%), the light penetrated deeper into the sparsely distributed plants (rainfed site), while light absorption in the more densely irrigated site was somewhat limited by the shadow by nearby plants. Therefore, light absorption was more effective in the rainfed site (due to higher specific absorption, fAPAR/chlorophyll — Peng et al., 2011) than in the irrigated site, thus resulting in higher VI values in the rainfed site.

In addition to the difference in water supply, the crop hybrids and field managements were also different during the 8 years of observation. Eight different cultivars of maize and three cultivars of soybean were grown in the 24 site-years, density of planting ranged from 52,000 to 84,012 plants/ha, and nitrogen applied ranged from 90 to 293 kg N/ha among the maize sites (Peng & Gitelson, 2011). From 2006 through 2008, site 1 was under the conservation–plow tillage operation while site 2 and site 3 were under no-till management. And the climatic conditions were quite different among the 8 years. For example, the mean monthly temperatures in June and July were warmer in 2001 and 2002 than in 2003. There were obvious dry periods during reproductive stages in 2001 and 2003 and during vegetative stages in 2005. In contrast, 2006, 2007 and 2008 were relatively wet years with no significant dry period (Suyker & Verma, 2010). All these differences existing among years and sites might cause the uncertainties of GPP estimation using a VI-PAR-based model.

To understand how models estimated GPP in different sites, we established the relationships of GPP vs. VI × PAR, with PAR_{in} and $PAR_{potential}$, for each site with samples taken from different years combined for irrigated maize (site 1: 2001, 2003, 2005 and 2007 and site 2: 2001, 2003, 2005 and 2007) and rainfed maize (site 3: 2001, 2003, 2005 and 2007), for irrigated soybean (site 2: 2002, 2004, 2006 and 2008) and rainfed soybean (site 3: 2002, 2004, 2006 and 2008), and then compared R^2, SE and CV for the difference ($PAR_{potential} - PAR_{in}$)/$PAR_{in}$<20% and ($PAR_{potential} - PAR_{in}$)/$PAR_{in}$<40% (Tables 2a and 2b). For two irrigated maize sites (site 1 and site 2), the accuracy of GPP estimation was almost the same. It means the difference in crop hybrids, planting densities and tillage operations only affected the accuracy of the model slightly. In both maize and soybean, the model accuracy for the rainfed site was somewhat lower than for irrigated site. For each year, the model was able to estimate GPP in the rainfed and irrigated sites very accurately (e.g., Fig. 6A for the data in 2003). However, the relationships for different years in the rainfed site deviated more from each other than in the irrigated site, thus resulting in

Table 2a
Determination coefficients (R^2), standard errors (SE) and coefficients of variation (CV) of GPP estimation in maize using WDRVI∗PAR with PAR_{in} and $PAR_{potential}$ for irrigated site 1 and site 2 and rainfed site 3, Mead, NE in 2001, 2003, 2005 and 2007. N is the number of samples used for developing the relationship.

GPP = VI∗PAR, maize		($PAR_{potential} - PAR_{in}$)/$PAR_{in}$<20%			($PAR_{potential} - PAR_{in}$)/$PAR_{in}$<40%		
	PAR	Site 1 irrigated (N = 260)	Site 2 irrigated (N = 281)	Site 3 rainfed (N = 270)	Site 1 irrigated (N = 386)	Site 2 irrigated (N = 392)	Site 3 rainfed (N = 375)
R^2	PAR_{in}	0.93	0.92	0.91	0.91	0.90	0.90
	$PAR_{potential}$	0.95	0.95	0.93	0.94	0.94	0.92
SE, gC/m²/d	PAR_{in}	2.21	2.37	2.18	2.52	2.68	2.43
	$PAR_{potential}$	1.94	1.92	2.00	2.04	2.13	2.20
CV, %	PAR_{in}	13.4	14.6	15.2	15.9	16.6	17.2
	$PAR_{potential}$	11.7	11.8	14.0	12.8	13.2	15.5

Table 2b
Determination coefficients (R^2), standard errors (SE) and coefficients of variation (CV) for GPP estimation in soybean using WDRVI∗PAR with PAR_{in} and $PAR_{potential}$ for site 2 and site 3, Mead, NE in 2002, 2004, 2006 and 2008. N is the number of samples used for developing relationship.

GPP = VI∗PAR, soybean		$(PAR_{potential} - PAR_{in})/PAR_{in} < 20\%$		$(PAR_{potential} - PAR_{in})/PAR_{in} < 40\%$	
	PAR	Site 2 irrigated (N = 248)	Site 3 rainfed (N = 244)	Site 2 irrigated (N = 352)	Site 3 rainfed (N = 348)
R^2	PAR_{in}	0.88	0.85	0.83	0.81
	$PAR_{potential}$	0.89	0.87	0.87	0.85
SE, $gC/m^2/d$	PAR_{in}	1.90	2.02	2.13	2.21
	$PAR_{potential}$	1.78	1.91	1.80	1.93
CV, %	PAR_{in}	19.0	20.0	21.9	24.5
	$PAR_{potential}$	17.8	21.1	18.5	21.5

somewhat higher estimation errors when developing a unified algorithm with samples from different years combined.

3.4. Relationships of EVI with ρ_{NIR} and ρ_{red}

It is interesting to note that there were more scattering of points from best-fit functions for products using EVI than those using other indices, especially for maize at moderate to high GPP (Fig. 3). To understand the reason for that, the relationships EVI vs. ρ_{NIR} and EVI vs. $(\rho_{NIR} - \rho_{red})$ were studied using data retrieved from 8-day composite MODIS products for both maize and soybean in three irrigated and rainfed fields from 2001 through 2008 (Fig. 7). Throughout the eight-year growing seasons, EVI was closely related to ρ_{NIR} with R^2 above 0.84, and this close relationship was observed in both maize and soybean, which are two different crop types with contrasting leaf structures and canopy architectures (Fig. 7A). It was especially pronounced for moderate to high vegetation density (as EVI exceeded 0.4) when red reflectance was small (below 4%) and almost invariant, and EVI was solely related to ρ_{NIR} that was above 30%. Thus, NIR reflectance was the main factor governing EVI for moderate to high vegetation density.

In both maize and soybean, the relationship EVI vs. $\rho_{NIR} - \rho_{red}$ was extremely close with R^2 above 0.98 (Fig. 7B). In reality, EVI behaved as a difference between NIR and the red reflectance, not as normalized difference (Fig. 7B). Since NIR reflectance plays the main role in EVI formulation and it may be affected by many factors (e.g., view angle, leaf orientations, canopy architecture), EVI tends to be noisier than the other normalized difference indices.

The strong relationship EVI vs. $(\rho_{NIR} - \rho_{red})$ explains much higher sensitivity of EVI than NDVI to moderate-to-high vegetation density, since light scattering (and, thus, ρ_{NIR}) increases with increase of vegetation density. This also helps to understand recent findings at three flux tower sites (Harvard Forest, Howland Forest and Morgan Monroe State Forest) that EVI was significantly affected by view angles (Sims et al., 2011). The authors found a substantial variation in the view angle sensitivity of EVI across seasons, and this variation was different for backscattering vs. forward scattering data.

3.5. Limitation of GPP model using PAR_{in}

The VI-PAR_{in}-based model is developed based on Monteith's model (Monteith, 1972, 1977), which assumes that for the same

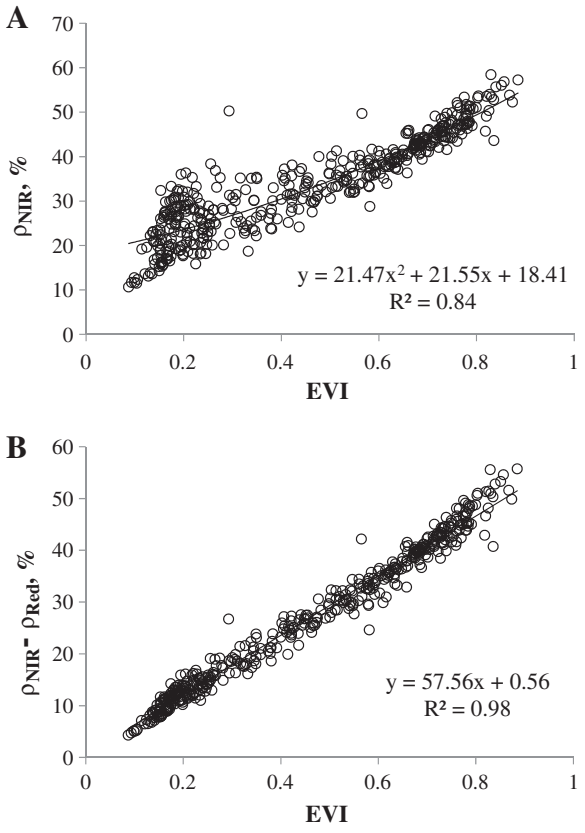

Fig. 7. Relationship of EVI vs. (A) NIR reflectance, ρ_{NIR}, and (B) difference between NIR and red reflectances, $\rho_{NIR} - \rho_{red}$, in irrigated and rainfed maize and soybean sites in Nebraska from 2001 through 2008. Reflectances and EVI were retrieved from 8-day composite MODIS data.

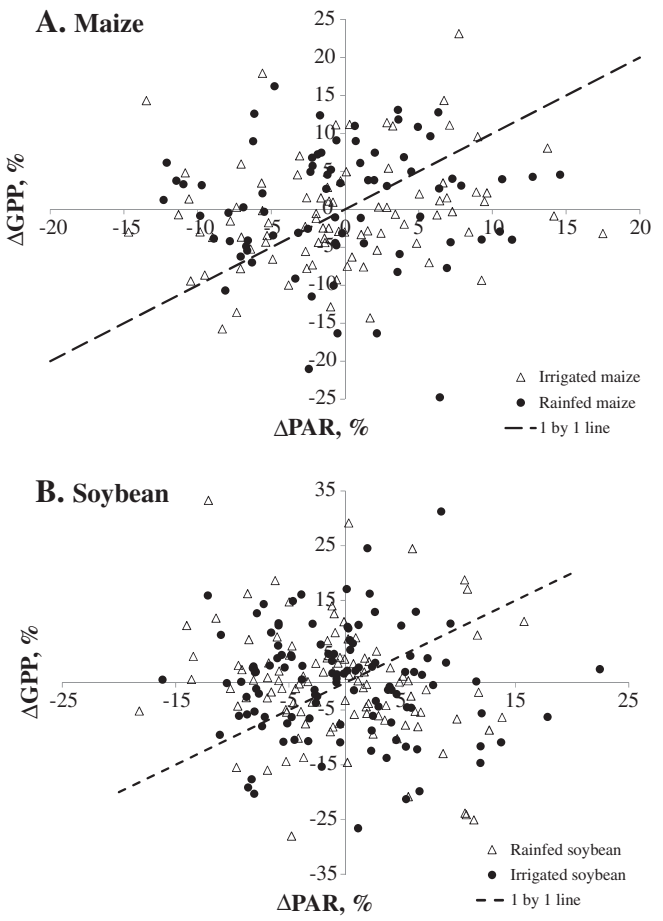

Fig. 8. Variation of GPP, ΔGPP, plotted versus variation of PAR_{in}, ΔPAR_{in}, for pairs of two consecutive events with equal crop Chl content/fAPAR for (A) irrigated and rainfed maize and (B) irrigated and rainfed soybean during 2001 through 2008.

fraction of absorbed photosynthetically active radiation, fAPAR, GPP linearly relates to PAR_{in} and that light use efficiency (LUE) is constant for the same crop species. However, some studies have shown that these assumptions do not hold in many cases (e.g., Suyker et al., 2005).

To investigate how variations of PAR_{in} and LUE affect GPP, daily available GPP and PAR_{in} data were used in conjunction with daily MODIS VI products. To analyze the response of GPP to variation of PAR_{in}, pairs of events with the same crop chlorophyll/fAPAR should be found. To meet this requirement, the pairs were selected as the difference in MODIS-retrieved VIs for the two events was below 1%. Thus, for each pair of events, the change in crop Chl content/fAPAR was minimal. Usually, such events appeared at two close dates (time interval was less than 3 days), so the crop physiological and phenological states in both events were quite similar. Pairs of events were also selected under conditions of low aerosol loadings when crop photosynthesis was not light limited: the difference $(PAR_{potential} - PAR_{in})/PAR_{potential}$ for each selected pair was below 20%. Therefore, assuming that fAPAR was the same for each pair, the variation of GPP was related only to variation of PAR_{in} and LUE. In total, 162 pairs data from maize fields (86 for irrigated sites and 76 for rainfed sites) and 220 pairs data from soybean sites (114 for irrigated fields and 106 for rainfed sites) were selected during the growing seasons 2001 through 2008.

For each pair, the GPP variation (ΔGPP) and PAR_{in} variation (ΔPAR_{in}) in a percentage were calculated and compared. According

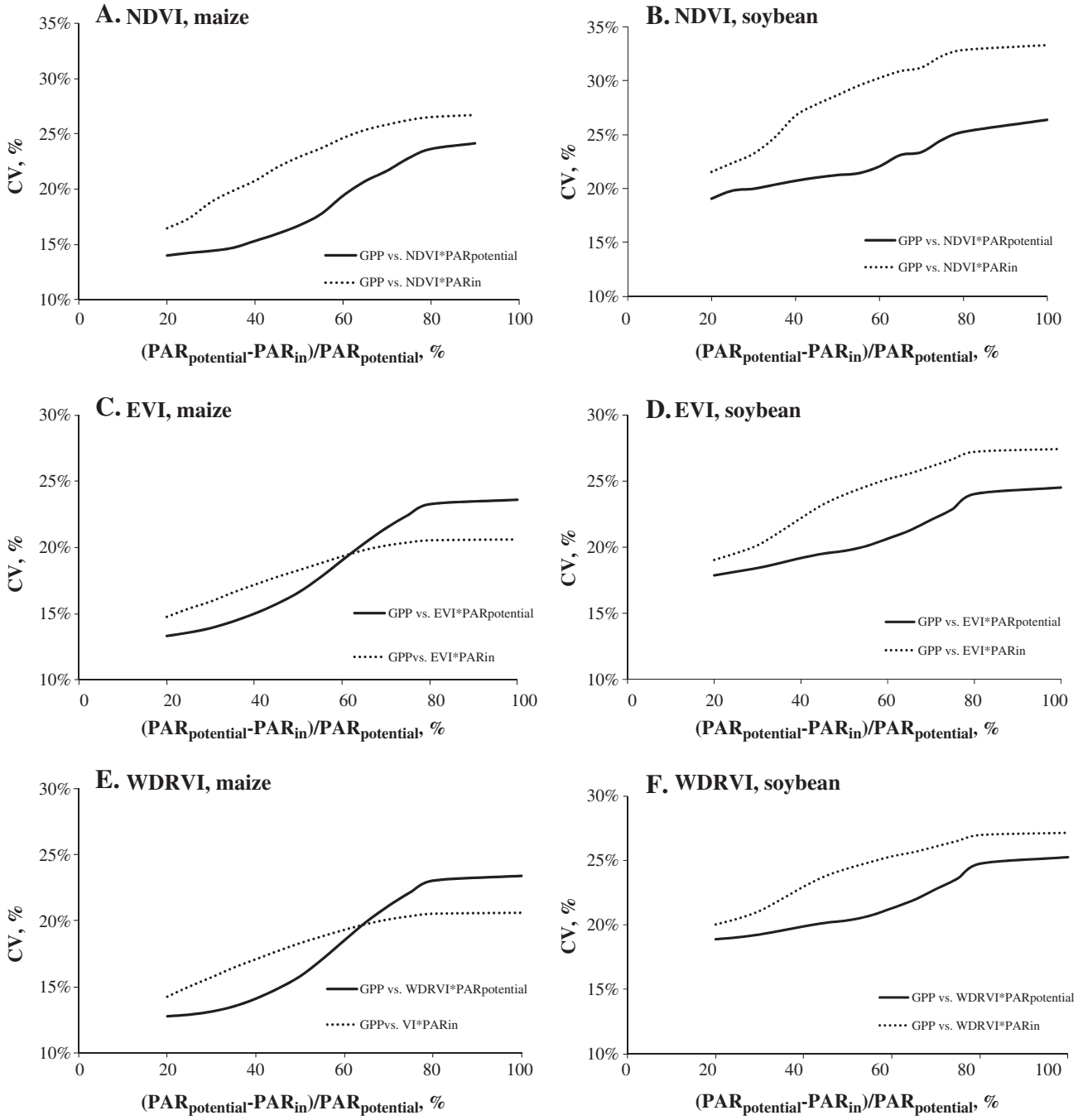

Fig. 9. Coefficients of variation of two GPP estimation models — $VI \times PAR_{in}$ and $VI \times PAR_{potential}$, plotted versus the difference, $(PAR_{potential} - PAR_{in})/PAR_{potential}$, for NDVI in maize (A) and soybean (B); EVI in maize (C) and soybean (D) and WDRVI in maize (E) and soybean (F).

to Monteith's model, for each pair (when crop fAPAR was invariant and LUE assumed to be a constant for the two events) ΔGPP should be equal to ΔPAR_{in}. However, for both irrigated and rainfed maize and soybean, it was a cluster of points (Fig. 8). The same pattern of ΔGPP vs. ΔPAR_{in} relationship was found when the difference $(PAR_{potential} - PAR_{in})/PAR_{potential}$ for each selected pair was below 40% (not shown). In the contrasting crop types (maize vs. soybean) under different water treatments (irrigated vs. rainfed), GPP did not follow PAR_{in}. For the same PAR_{in} ($\Delta PAR_{in} = 0$), GPP varied widely. Thus, when crop fAPAR and PAR_{in} did not change, other factors (e.g., temperature, soil moisture, and humidity) did affect GPP (e.g., Suyker and Verma, 2010). As PAR_{in} decreases/increases, GPP may almost remain the same. Some research has shown that crop could adjust itself to variation of the incoming radiation, thus not causing immediate changes of GPP. For example, photo-protection mechanisms were likely invoked to prevent excess light damages to photosynthetic processes (e.g., Bjorkman & Powles, 1984; Kasahara et al., 2002). As PAR_{in} fluctuates with daily weather conditions, there are quite a lot of uncertainties in GPP variation, which may relate to many factors such as crop physiological status and light climate inside the canopy that affect absorbed PAR and LUE. Therefore, the use of PAR_{in} in the model may introduce noise and unpredictable uncertainties in GPP estimation. In contrast, using $PAR_{potential}$ reduced, to some degree, such noise of the model.

To compare efficiency of using PAR_{in} and $PAR_{potential}$ in the models, CV of the models with PAR_{in} and $PAR_{potential}$ was plotted versus difference $(PAR_{potential} - PAR_{in})/PAR_{potential}$ (Fig. 9). When the difference $(PAR_{potential} - PAR_{in})/PAR_{potential}$ increased (as more and more data taken under cloudy or hazy weather conditions were included), the accuracy of both models decreased. However, for all indices tested, NDVI, EVI and WDRVI, the models using $PAR_{potential}$ had smaller CV values for the whole range of PAR_{in} variation in soybean and with the difference well above 60% for maize. In maize, as the difference between $PAR_{potential}$ and PAR_{in} exceeded 60%, the discrepancy between GPP estimates by a product of $VI \times PAR_{potential}$ and measured GPP increased, so the use of PAR_{in} in the models is preferable. For soybean data, the model with PAR_{in} was consistently inferior to the model with $PAR_{potential}$. Thus, with all three MODIS-retrieved vegetation indices in both maize and soybean, the model using $PAR_{potential}$ appeared to be more accurate for GPP estimation during conditions when the difference $(PAR_{potential} - PAR_{in})/PAR_{potential}$ was below 60%.

4. Conclusions

The model using the product of MODIS-retrieved vegetation indices and potential PAR was able to accurately estimate GPP in irrigated and rainfed croplands. EVI and WDRVI were accurate in estimating GPP with standard error (SE) below 2.15 $gC/m^2/d$ and coefficient of variation (CV) of less than 15.2% for maize, and SE below 1.75 $gC/m^2/d$ and CV less than 20.1% for soybean. The GPP estimation model with $PAR_{potential}$ was more accurate than the models with PAR_{in} or SW under a condition when difference between PAR_{in} and $PAR_{potential}$ was below 60%. This model was quite sensitive to GPP variation in both irrigated and rainfed crops where total chlorophyll content is closely tied to the seasonal dynamic of GPP. The approach allows for accurate high temporal resolution monitoring of crop GPP using solely MODIS 250 m data.

This study provides a tool for accurate estimation of crop GPP using a product of MODIS-retrieved VI and $PAR_{potential}$. However, it is recognized that this model does not take into account GPP variation that was not accompanied by crop Chl changes, which may be caused by short-term (minutes to hours) stresses. $PAR_{potential}$ varies in different geographic locations as latitude changes. It is not clear how location difference affects GPP estimation model that uses $PAR_{potential}$, and whether algorithms calibrated in one geographic region could be used for very different latitudes with no re-parameterization. Therefore, it is essential to test accuracy of the GPP estimation model, presented in this study, for other geographic locations, as well as for other crop types. In addition, the in-depth analysis of GPP response to PAR_{in} variation needs to be further explored.

In this paper, maximal values of measured PAR_{in} as a surrogate for $PAR_{potential}$ have been used. The next step is to calculate $PAR_{potential}$ using radiative transfer approaches and to test the model using MODIS data with calculated daily $PAR_{potential}$. Having 12 years GPP data at three Nebraska AmeriFlux sites (2001–2012) will allow comprehensive testing of the model based solely on remotely sensed data.

Acknowledgments

This research was supported by NASA NACP grant No. NNX08AI75G and partially by the U.S. Department of Energy: (a) EPSCoR program, Grant No. DE-FG-02-00ER45827 and (b) Office of Science (BER), Grant No. DE-FG03-00ER62996. We sincerely appreciate the support and the use of facilities and equipment provided by the Center for Advanced Land Management Information Technologies (CALMIT) and CALMIT leader Dr. D.C. Rundquist and data from UNL Carbon Sequestration Program led by Dr. S. Verma.

References

Ahl, D. E., Gower, S. T., Mackay, D. S., Burrows, S. N., Norman, J. M., & Diak, G. R. (2004). Heterogeneity of light use efficiency in a northern Wisconsin forest: implications for modeling net primary production with remote sensing. *Remote Sensing of Environment*, *93*, 168–178.

Almond, S., Boyd, D. S., Dash, J., Curran, P. J., Hill, R. A., & Foody, G. M. (2010). Estimating terrestrial gross primary productivity with the Envisat Medium Resolution Imaging Spectrometer (MERIS) Terrestrial Chlorophyll Index (MTCI). *Geoscience and Remote Sensing Symposium (IGARSS), 2010 IEEE International*, 4792–4795, Honolulu, HI.

Anderson, M. A., Norman, J. M., Meyers, T. P., & Diak, G. R. (2000). An analytical model for estimating canopy transpiration and carbon assimilation fluxes based on canopy light-use efficiency. *Agricultural and Forest Meteorology*, *100*, 265–289.

Asrar, G., Fuchs, M., Kanemasu, E. T., & Hatfield, J. H. (1984). Estimating absorbed photosynthetic radiation and leaf area index from spectral reflectance in wheat. *Agronomy Journal*, *76*, 300–306.

Bjorkman, O., & Powles, S. B. (1984). Inhibition of photosynthetic reactions under water stress: Interaction with light level. *Planta*, *161*, 490–504.

Boyd, D. S., Almod, S., Dash, J., Curran, P. J., Hill, R. A., & Foody, G. M. (2012). Evaluation of Envisat MERIS terrestrial chlorophyll index-based models for the estimation of terrestrial gross primary productivity. *Geoscience and Remote Sensing Letters*, *9*(3), 457–461.

Cassman, K. G., & Wood, S. (2005). Cultivated systems. *Millennium ecosystem assessment: Global ecosystem assessment report on conditions and trends* (pp. 741–789). Washington, DC: Island Press.

Fang, H. (2009). *Readme document for North America Land Data Assimilation System Phase 2 (NLDAS-2) Products.* Goddard Earth Sciences Data and Information Service Center (Available at:, http://hydro1.sci.gsfc.nasa.gov/data/s4pa/NLDAS/README.NLDAS2.pdf)

Gamon, J. A., Penuelas, J., & Field, C. B. (1992). A narrow waveband spectral index that tracks diurnal changes in photosynthetic efficiency. *Remote Sensing of Environment*, *4*, 35–44.

Garbulsky, M. F., Penuelas, J., Gamon, J., Inoue, Y., & Filella, L. (2011). The photochemical reflectance index (PRI) and the remote sensing of leaf, canopy and ecosystem radiation use efficiencies: A review and meta-analysis. *Remote Sensing of Environment*, *115*(2), 281–297.

Gitelson, A. A. (2004). Wide dynamic range vegetation index for remote quantification of biophysical characteristics of vegetation. *Journal of Plant Physiology*, *161*(2), 165–173.

Gitelson, A. A., Peng, Y., Masek, J. G., Rundquist, D. C., Verma, S. B., Suyker, A., Baekr, J. M., Hatfield, J. L., & Meyers, T. (2012). Remote estimation of crop gross primary production with Landsat data. *Remote Sensing of Environment*, *121*, 404–414.

Gitelson, A. A., Verma, S. B., Viña, A., Rundquist, D. C., Keydan, G., Leavitt, B., Arkebauer, T. J., Burba, G. G., & Suyker, A. E. (2003). Novel technique for remote estimation of CO_2 flux in maize. *Geophysical Research Letter*, *30*(9), 1486, http://dx.doi.org/10.1029/2002GL016543

Gitelson, A. A., Viña, A., Masek, J. G., Verma, S. B., & Suyker, A. E. (2008). Synoptic monitoring of gross primary productivity of maize using Landsat data. *IEEE Geoscience and Remote Sensing Letters*, *5*, 2, http://dx.doi.org/10.1109/LGRS.2008.915598

Gitelson, A. A., Viña, A., Verma, S. B., Rundquist, D. C., Arkebauer, T. J., Keydan, G., Leavitt, B., Ciganda, V., Burba, G. G., & Suyker, A. E. (2006). Relationship between gross primary production and chlorophyll content in crops: Implications for the synoptic monitoring of vegetation productivity. *Geophysical Research Letter*, *111*(D08S11), http://dx.doi.org/10.1029/2005JD006017

Harris, A., & Dash, J. (2010). The potential of the MERIS Terrestrial chlorophyll Index for carbon flux estimation. *Remote Sensing of Environment*, *114*, 1856–1862.

Huete, A. R., Liu, H. Q., Batchily, K., & van Leeuwen, W. (1997). A comparison of vegetation indices global set of TM images for EOS-MODIS. *Remote Sensing of Environment*, *59*, 440–451.

Kanemasu, E. T. (1974). Seasonal canopy reflectance patterns of wheat, sorghum, and soybean. *Remote Sensing of Environment*, *3*, 43–47.

Kasahara, M., Kagawa, T., Oikawa, K., Suetsugu, N., Miyao, M., & Wada, M. (2002). Chloroplast avoidance movement reduces photodamage in plants. *Nature*, *420*, 829–832.

Kotchenova, S. Y., & Vermote, E. F. (2007). Validation of a vector version of the 6S radiative transfer code for atmospheric correction of satellite data. Part II. Homogeneous Lambertian and anisotropic surfaces. *Applied Optics*, *46*(20), 4455–4464.

Liu, J., Chen, J. M., Cihlar, J., & Park, W. M. (1997). A process-based boreal ecosystem productivity simulator using remote sensing inputs. *Remote Sensing of Environment*, *62*, 158–175.

Lyapustin, A. (2003). Interpolation and Profile Correction (IPC) method for shortwave radiative transfer in spectral intervals of gaseous absorption. *Journal of the Atmospheric Sciences*, *60*, 865–871.

Malmstrom, C. M., Thompson, M. V., Juday, G. P., Los, S. O., Randerson, J. T., & Field, C. B. (1997). Interannual variation in global-scale net primary production: Testing model estimates. *Global Biogeochemical Cycles*, *11*, 367–392.

Medina, E., & Lieth, H. (1964). Die Beziehungen zwischen Chlorophyllgehalt, assimilierender Flaeche und Trockensubstanzproduktion in einigen Pflanzengemeinschaften [The relationships between chlorophyll content, assimilating area and dry matter production in some plant communities]. *Beitraege zur Biologie der Pflanzen*, *40*, 451–494.

Monteith, J. L. (1972). Solar radiation and productivity in tropical ecosystems. *Journal of Applied Ecology*, *9*, 744–766.

Monteith, J. L. (1977). Climate and the efficiency of crop production in Britain. *Philosophical Transactions of the Royal Society of London*, *281*, 277–294.

Nguy-Robertson, A. L., Gitelson, A. A., Peng, Y., Viña, A., Arkebauer, T. J., & Rundquist, D. C. (2012). Green leaf area index estimation in maize and soybean: Combining vegetation indices to achieve maximal sensitivity. *Agronomy Journal*, *104*(5), 1336–1347.

Osborne, B. A., & Raven, J. A. (1986). Light absorption by plants and its implications for photosynthesis. *Biological Reviews*, *61*(1), 1–60, http://dx.doi.org/10.1111/j.1469-185X.1986.tb00425.x

Peng, Y. (2012). *Chlorophyll-based approach for remote estimation of crop gross primary production: From in situ measurements to satellite imagery*. ETD Collection for University of Nebraska-Lincoln (AAI3518154).

Peng, Y., & Gitelson, A. A. (2011). Application of chlorophyll-related vegetation indices for remote estimation of maize productivity. *Agricultural and Forest Meteorology*, *151*, 1267–1276.

Peng, Y., Gitelson, A. A., Keydan, G., Rundquist, D. C., & Moses, W. (2011). Remote estimation of gross primary production in maize and support for a new paradigm based on total crop chlorophyll content. *Remote Sensing of Environment*, *115*, 978–989.

Potter, C. S., Randerson, J. T., Field, C. B., Matson, P. A., Vitousek, P. M., Mooney, H. A., & Klooster, S. A. (1993). Terrestrial ecosystem production: A process model based on global satellite and surface data. *Global Biogeochemical Cycles*, *7*(4), 811–841.

Rouse, J. W., Haas, R. H., Jr., Schell, J. A., & Deering, D. W. (1974). Monitoring vegetation systems in the Great Plains with ERTS. *NASA SP-351, Third ERTS-1 Symposium NASA Washington DC*, *1*. (pp. 309–317).

Ruimy, A., Saugier, B., & Dedieu, G. (1994). Methodology for the estimation of terrestrial net primary production from remotely sensed data. *Journal of Geophysical Research*, *99*, 5263–5283.

Running, S. W., Nemani, R. R., Heinsch, F. A., Zhao, M. S., Reeves, M., & Hashimoto, H. (2004). A continuous satellite-derived measure of global terrestrial primary production. *Bioscience*, *54*, 547–560.

Sakamoto, T., Gitelson, A. A., Wardlow, B. D., Verma, S. B., & Suyker, A. E. (2011). Estimating daily gross primary production of maize based only on MODIS WDRVI and shortwave radiation data. *Remote Sensing of Environment*, *115*, 3091–3101.

Sakamoto, T., Van Nguyen, N., Kotera, A., Ohno, H., Ishitsuka, N., & Yokozawa, M. (2007). Detecting temporal changes in the extent of annual flooding within the Cambodia and the Vietnamese Mekong Delta from MODIS time-series imagery. *Remote Sensing of Environment*, *109*, 295–313.

Sakamoto, T., Wardlow, B. D., Gitelson, A. A., Verma, S. B., Suyker, A. E., & Arkebauer, T. J. (2010). A two-step filtering approach for detecting maize and soybean phenology with time-series MODIS data. *Remote Sensing of Environment*, *114*, 2146–2159.

Sims, D. A., Rahman, A. F., Vermote, E. F., & Jing, Z. (2011). Seasonal and inter-annual variation in view angle effects on MODIS vegetation indices at three forest sites. *Remote Sensing of Environment*, *115*, 3112–3120.

Suyker, A. E., & Verma, S. B. (2010). Coupling of carbon dioxide and water vapor exchanges of irrigated and rainfed maize–soybean cropping systems and water productivity. *Agricultural and Forest Meteorology*, *150*, 553–563.

Suyker, A. E., Verma, S. B., Burba, G. G., & Arkebauer, T. J. (2005). Gross primary production and ecosystem respiration of irrigated maize and irrigated soybean during a growing season. *Agricultural and Forest Meteorology*, *131*, 180–190.

Thenkabail, P. S., Schull, M., & Turral, H. (2005). Ganges and Indus river basin land use/land cover (LULC) and irrigated area mapping using continuous streams of MODIS data. *Remote Sensing of Environment*, *95*, 317–341.

Turner, D. P., Urbanski, S., Bremer, D., Wofsy, S., Meyers, T., Gower, S. T., et al. (2003). A cross-biome comparison of daily light use efficiency for gross primary production. *Global Change Biology*, *9*, 383–395.

Verma, S. B., Dobermann, A., Cassman, K. G., Walters, D. T., Knops, J. M., Arkebauer, T. J., Suyker, A. E., Burba, G. G., Amos, B., Yang, H., Ginting, D., Hubbard, K. G., Gitelson, A. A., & Walter-Shea, E. A. (2005). Annual carbon dioxide exchange in irrigated and rainfed maize-based agroecosystems. *Agricultural and Forest Meteorology*, *131*, 77–96.

Vermote, E. F., Tanré, D., Deuzé, J. L., Herman, M., & Morcrette, J. J. (1997). Second simulation of the satellite signal in the solar spectrum: An overview. *IEEE Transactions on Geoscience and Remote Sensing*, *35*(3), 675–686.

Viña, A., & Gitelson, A. A. (2005). New developments in the remote estimation of the fraction of absorbed photosynthetically active radiation in crops. *Geophysical Research Letters*, *32*, L17403, http://dx.doi.org/10.1029/2005GL023647

Viña, A., Gitelson, A. A., Nguy-Robertson, A. L., & Peng, Y. (2011). Comparison of different vegetation indices for the remote assessment of green leaf area index of crops. *Remote Sensing of Environment*, *115*, 3468–3478.

Whittaker, R. H., & Marks, P. L. (1975). Methods of assessing terrestrial productivity. In H. Lieth, & R. H. Whittaker (Eds.), *Primary productivity of the biosphere. Ecological studies*, *14*. (pp. 55–118): Springer-Verlag.

Wood, S., Sebastian, K., & Scherr, S. J. (2000). *Pilot analysis of global ecosystems (agroecosystems)*, *110*, Washington, DC: International Food Policy Research Institute and World Resources Institute.

Wu, C., Chen, J. M., & Huang, N. (2011). Predicting gross primary production from the enhanced vegetation index and photosynthetically active radiation: Evaluation and calibration. *Remote Sensing of Environment*, http://dx.doi.org/10.1016/j.rse.2011.08.006

Wu, C., Niu, Z., & Gao, S. (2010). Gross primary production estimation from MODIS data with vegetation index and photosynthetically active radiation in maize. *Journal of Geophysical Research*, *115*, D12127, http://dx.doi.org/10.1029/2009JD013023

Wu, C., Niu, Z., Tang, Q., Huang, W., Rivard, B., & Feng, J. (2009). Remote estimation of gross primary production in wheat using chlorophyll-related vegetation indices. *Agricultural and Forest Meteorology*, *149*, 1015–1021.

Xiao, X., Boles, S., Frolking, S., Li, C., Babu, J. Y., Salas, W., & Moore, B. (2006). Mapping paddy rice agriculture in South and Southeast Asia using multitemporal MODIS images. *Remote Sensing of Environment*, *100*, 95–113.

Xiao, X., Hollinger, D., Aber, J., Goltz, M., Davidson, E. A., Zhang, Q., & Moore, B. (2004a). Satellite-based modeling of gross primary production in an evergreen needleleaf forest. *Remote Sensing of Environment*, *89*(4), 519–534.

Xiao, X., Zhang, Q., Braswell, B., Urbanski, S., Boles, S., Wofsy, S., Moore, B., & Ojima, D. (2004b). Modeling gross primary production of temperate deciduous broadleaf forest using satellite images and climate data. *Remote Sensing of Environment*, *2004*, 256–270.

Xiao, J., Zhang, Q., Law, B., Baldocchi, D. D., Chen, J., Richardson, A. D., Melillo, J. M., et al. (2011). Assessing net ecosystem carbon exchange of U.S. terrestrial ecosystems by integrating eddy covariance flux measurements and satellite observations. *Agriculture and Forest Meteorology*, *151*, 60–69.

Xu, L., & Baldocchi, D. D. (2003). Seasonal trend of photosynthetic parameters and stomatal conductance of blue oak (*Quercus douglasii*) under prolonged summer drought and high temperature. *Tree Physiology*, *23*, 865–877.

Yuan, W., Liu, S., Zhou, G. S., Zhou, G., Tieszen, L. L., Baldocchi, D., et al. (2007). Deriving a light use efficiency model from eddy covariance flux data for predicting daily gross primary production across biomes. *Agricultural and Forest Meteorology*, *143*, 189–207.